

# THE SHEAR STRENGTH OF PRESTRESSED BRICKWORK I AND T SECTIONS

N ROUMANI B.Sc., M.Sc. and

M E PHIPPS B.Sc. Tech, Ph.D., C.Eng., M.I.C.E., M.I. Struct.E.,  
University of Manchester Institute of Science and Technology, England.

## ABSTRACT

The paper presents the results of a programme of experiments on the shear strength of prestressed brickwork beams with I and T shaped cross sections. Prestress was applied using unbonded tendons which were placed at the sides of the webs and anchored at the ends of the beams. The main objectives were to assess the influence of the shear span/depth ratio, the depth and shape of the section, the amount of prestress and concentric and eccentric prestress.

The modes of failure observed in the tests and the effects the various parameters have on the shear behaviour of the beams are described. An expression, based on the principal tension theory, is developed for the diagonal cracking of the beams. The formation of inclined cracking in the web of the section transforms the beam into a complex structure and consequently the beam's ultimate strength has been assessed empirically.

Equations are presented which can be used safely in design to assess shear strength at the cracking and collapse stages.

## NOTATION

$a$	length of shear span	
$b$	width of section being considered	
$d$	overall depth of beam	
$A_b$	cross-sectional area of beam	
$Z_b$	section modulus at soffit of beam	
$A\bar{y}/I_b$	shear stress coefficient at centroid of section	
$M$	flexural cracking moment	
$M^c$	diagonal cracking moment	
$M^u$	ultimate moment	
$P_e$	effective prestress force in tendons	
$P^u$	force in tendons at ultimate	
$V^c$	shear force at onset of flexural cracking	
$V^{cr}$	shear force at diagonal cracking	
$V^u$	shear force at ultimate	
$\sigma_b$	stress at soffit of beam due to prestress	$\frac{P_e}{A_b}$
$\sigma_p$	average stress in brickwork due to prestress	
$\sigma_{pu}$	notional ultimate stress in brickwork	$\frac{P^u}{A_b}$
$\sigma_{tf}$	principal tensile stress at failure	
$\tau_f$	shear stress at failure at centroid of section	
$f_{kt}$	flexural tensile strength of masonry	

## 1. INTRODUCTION

The tests reported in this paper form the second part of an experimental investigation aimed at examining the shear strength of prestressed brickwork sections. The sections chosen, I and T shapes, are those that represent closely the walls which, because of their efficient structural shape, benefit

most from the application of prestress, namely diaphragm and fin walls.

An earlier paper<sup>1</sup> described the first part of the study on nine I section beams and gave a preliminary account of the effects of prestress level and shear span/beam depth ratio on shear strength. This paper reports on tests on a further five I section beams and one T section beam and presents together the results of all fifteen tests.

With a view to formulating design proposals for the shear strength of brickwork sections at cracking and collapse the experimental objectives were:

1. to provide information on the influences of prestress level and shear span/beam depth ratio,
2. to study the effect of change in beam depth,
3. to examine the effect of change of section shape and eccentricity of prestress by the use of a T section beam,
4. to categorise the modes of failure.

## 2. EXPERIMENTS

Six full sized prestressed brickwork beams were built and tested under three point loading. Five of the beams were I shaped in cross-section and one was T shaped. The flange width in all the tests was kept the same at 670 mm. Three of the I beams, D1, D2 and D3, (Series D) together with the T beam, F1, (Series F) had an overall depth of 440 mm, identical to the previously tested beams<sup>1</sup> (Series A, B and C) with lengths varying from 3.0 to 4.0 m. The other two I beams, E1 and E2, (Series E) were 665 mm deep and 4.5 m in length, Fig. 1.

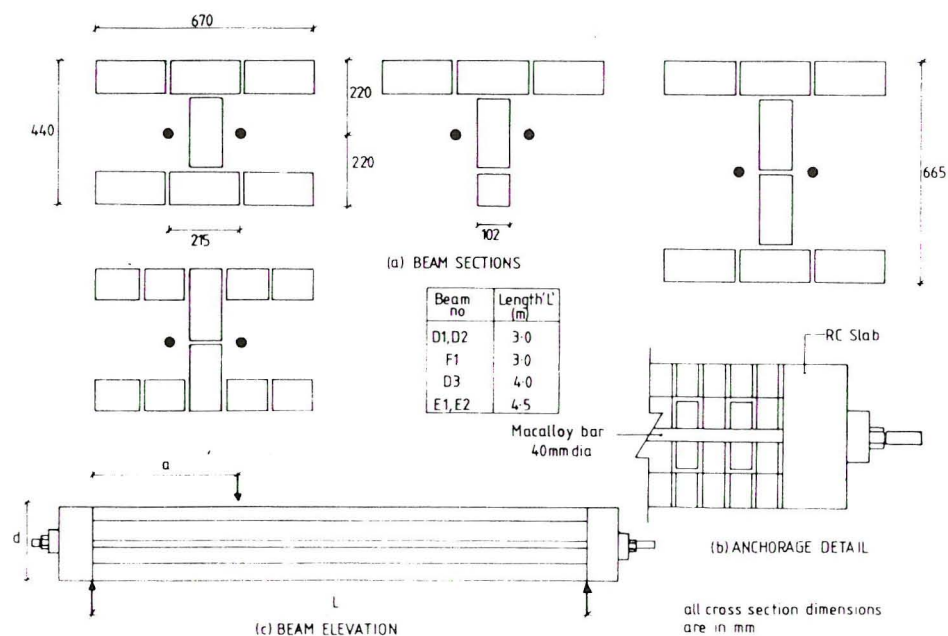


Figure 1. Detail of test beams

## 2.1 Construction of the beams

The beams were constructed vertically as columns, prestressed and then turned horizontally. Reinforced concrete slabs were used as end blocks to transfer the load from the prestressing bars to the brickwork. The bricks used were London Brick Company Fletton Class III. The mortar was a nominal 1:1:6, batched by weight.

When the beams were at least 28 days old, they were each prestressed with two 40 mm Macalloy high tensile steel bars. The tendons were placed along the centroidal axis of the I beams and along the mid-depth of the T beam, Fig. 1.

## 2.2 The test procedure

Since the beams were all tested under three point loading, it was possible to obtain two results from each beam by testing both ends. Once one end of a beam was loaded up to first cracking, it was then strengthened by a series of 'straps' enabling the other end of the beam to be tested up to first cracking and then on to ultimate. For beam D3 it was possible to carry out three tests.

Measurement of beam deformation and load were required at ultimate and beyond so an apparatus was used which was stiff enough to prevent unstable failures. Load was applied in increments of 2 - 3 kN and five minutes was allowed before logging the gauge outputs at each loading stage.

## 2.3 The test programme

2.3.1 The shallow I beams, D1, D2, D3 (440 mm deep). Four tests, D1-T2, D2-T1, D3-T1 and D3-T2, were carried out at a level of prestress on the masonry of approximately  $1.6 \text{ N/mm}^2$ . The shear span/beam depth ratio,  $a/d$ , was varied from 0.5 to 1.0 to 4.5, Table 1. These tests combined with three similar tests of Series B and C with  $a/d$  ratios of 1.5, 1.75 and 3.0 were used to define the influence  $a/d$  has on shear strength for one particular level of prestress. The testing apparatus did not have the capacity to reach ultimate when  $a/d = 0.5$  so a fifth test, D3-T3, was carried out at  $a/d = 1.0$  and a prestress level of  $3.0 \text{ N/mm}^2$ . Two tests, D1-T1 and D2-T2, had open perpendicular joints along the shear span under test, Figure 2. This was done, in part, to simulate perpendicular cracking in the web that occurred in the beams of Series A (this cracking was confined to the ends of the beams and was caused by the use of end blocks that were too flexible) but the tests also had the merit of investigating the effect of badly filled perpendicular joints.

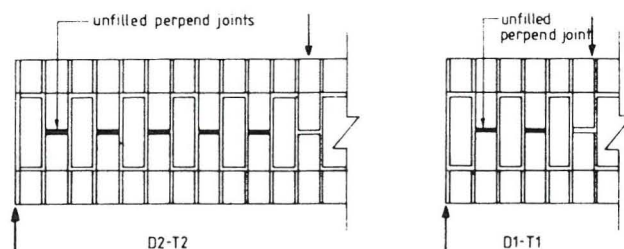


Figure 2.



2.3.2 The deeper I beams, E1 and E2, (665 mm deep). With the prestress on the masonry varying from approximately  $0.5 \text{ N/mm}^2$  to  $3.0 \text{ N/mm}^2$ , the four tests E1-T1, E1-T2, E2-T1 and E2-T2 were carried out at a constant  $a/d$  ratio of 2.0. The four tests compare with a similar four tests on shallow, 440 mm deep, beams reported in Series B and C.

2.3.3 The T beam, F1. This was the only eccentrically prestressed beam of all the beams tested. In the first test, F1-T1, the beam was centrally loaded resulting in  $a/d$  ratio of 3.44 on each side of the load point. For the second test, F1-T2, the  $a/d$  ratio was reduced to a value of 1.48 with the initial prestressing force kept at approximately the same level.

## 2.4 Modes of failure

The tests identified four distinct types of failure, Types II, III, IV and V, Figure 3. Failure Type I in Figure 3 has been shown by other work<sup>2</sup> to be typical of flexural failures and it is added to the shear failures II to V for completeness.

2.4.1 Type I, flexural failure. With tendons that are unbonded to the masonry, initial flexural tensile cracking transforms the beam into a tied arch. Providing there is sufficient steel area in the tendons, final collapse is brought about by crushing of the material in the compression zone (the crown of the arch).

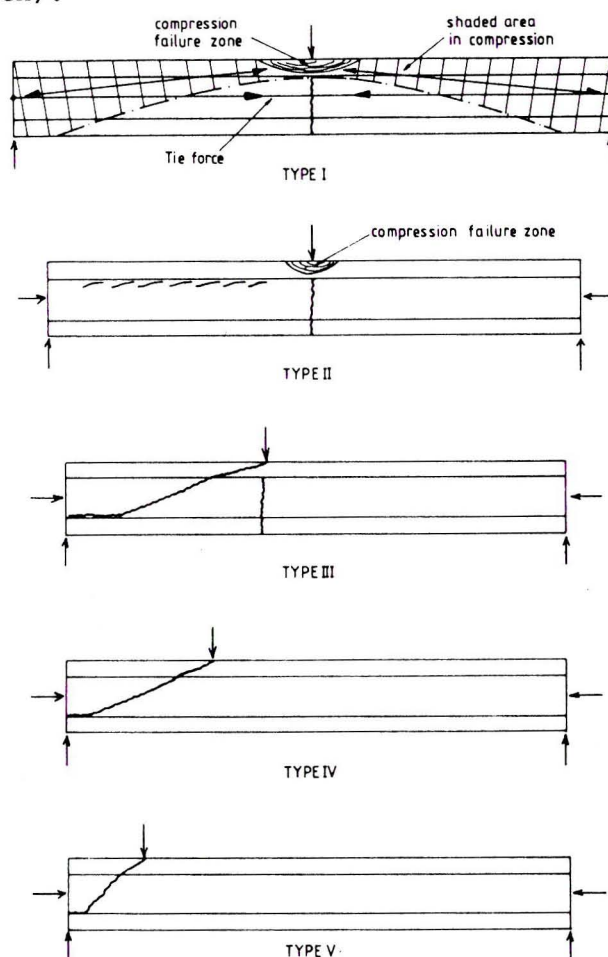


Figure 3.

Failure  
modes

2.4.2 Types II and III, shear failures. These two types of shear failure occur after flexural tensile cracking has taken place.

For Type II the integrity of the section is impaired by a series of cracks through the web at the web/flange intersection. The cracks develop at loads sufficiently high to cause some crushing of the brickwork near the load point.

For Type III inclined cracks develop independently of the flexural crack. The shear crack changes the behaviour of the beam quite dramatically, the deflection profile changing from single to double curvature, Figure 4. Failure appears as a shearing of the compression flange, or part of it, along an inclined plane.

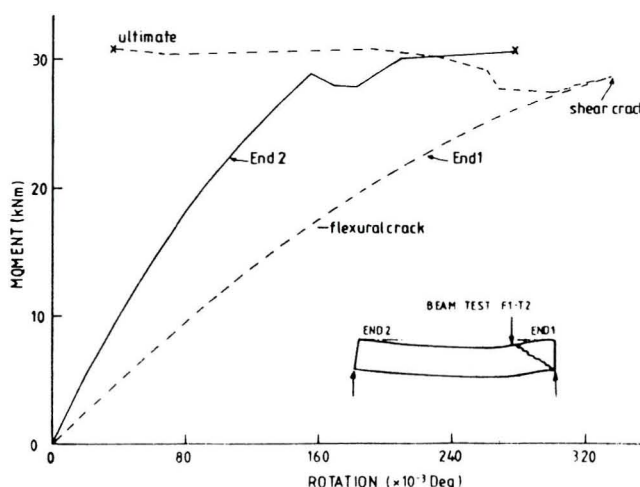


Figure 4. Moment - Rotation Curves

2.4.3 Types IV and V, shear failures. Here web shear cracks form before the flexural tensile strength of the masonry is reached.

For  $a/d$  ratios  $\geq 2.0$ , Type IV, the shear cracks are inclined at  $20^\circ$  to  $30^\circ$  to the longitudinal axis of the beam. The development of these cracks in most cases started at positions below or near to the centroidal axis of the beam, usually in the middle of the shear span. Collapse was due to the progressive penetration of the inclined cracks into the compression flange preceded by the formation of tensile cracks through the compression flange at the web/flange intersection.

When the  $a/d$  ratio is less than 1.5, Type V, the diagonal cracks form along a line joining the load and reaction points and consequently the cracks are inclined at much steeper angles.

### 3. TEST RESULTS

The average brick strength was  $9.5 \text{ N/mm}^2$  (frogs unfilled) and  $25 \text{ N/mm}^2$  (frogs filled). The 28 day mortar strength of 75 mm test cubes was  $8.0 \text{ N/mm}^2$ . To determine the compressive strength of the brickwork  $215 \times 215 \times 215$  prism cubes were tested. The average strength obtained was  $14 \text{ N/mm}^2$ . The results from the six beam tests are given in Table 1. Table 2 shows the results from test series A, B and C of reference 1. It will be noted that not all the beam tests were carried out to ultimate.

Test No.	a/d	$\sigma_p$ N/mm <sup>2</sup>	$V_c$ kN	$M_c$ kN-m	$V_{cr}$ kN	$M_{cr}$ kN-m	$V_u$ kN	$M_u$ kN-m	$\frac{V_u}{V_c}$	$\frac{V_u}{V_{cr}}$	$\frac{P_u}{P_e}$	Type of Failure
D1-T1**1.0	1.6	-	-	-	84.9	37.4	-	-	-	-	-	V
D1-T2	1.0	1.63	-	-	82.7	36.4	-	-	-	-	-	V
D2-T1	1.0	1.6	-	-	83.0	36.5	123.6	54.5	-	1.49	1.27	V
D2-T2**1.96	1.96	-	-	-	30.4	26.1	62.3	54.8	-	2.04	1.13	IV
D3-T1	4.52	1.07	17.5	34.8	29	57.6	29	57.6	1.66	1.0	1.25	III
D3-T2	0.5	1.62	-	-	156.6*	34.5	-	-	-	-	-	V
D3-T3	1.0	2.96	-	-	101	44.4	142	62.5	-	1.4	-	V
E1-T1	2.0	0.56	17.5	23.3	47.8	63.6	51.2	68.1	2.93	1.07	2.42	III
E1-T2	2.0	1.53	-	-	45.4	60.4	58.1	77.3	-	1.28	1.14	IV
E2-T1	2.0	1.87	-	-	42.7	56.8	65.7	87.4	-	1.54	1.10	IV
E2-T2	2.0	2.93	-	-	59.3	78.9	87.4	116.2	-	1.47	1.01	IV
F1-T1	3.44	2.70 <sup>†</sup>	10.94	16.6	-	-	35.3	53.5	3.23	-	2.89	II
F1-T2	1.48	3.0 <sup>†</sup>	25.9	16.85	44.0	28.6	47.1	30.6	1.82	1.07	1.61	III

<sup>†</sup> Comp stress at soffit of beam

\*\* Beam tests with unfilled perpend joints

\* Test stopped

Table 1. Test results of Series D, E and F

Test No.	a/d	$\sigma_p$ N/mm <sup>2</sup>	$V_c$ kN	$M_c$ kN-m	$V_{cr}$ kN	$M_{cr}$ kN-m	$V_u$ kN	$M_u$ kN-m	$\frac{V_u}{V_c}$	$\frac{V_u}{V_{cr}}$	$\frac{P_u}{P_e}$	Type of Failure
A3-T2	1.5	1.6	-	-	48.0	31.7	-	-	-	-	-	V
A1-T1	2.0	1.59	-	-	28.3	24.9	-	-	-	-	-	IV
A1-T2	2.0	1.59	-	-	27.9	24.6	-	-	-	-	-	IV
A2-T1	2.5	1.59	-	-	26.6	29.3	-	-	-	-	-	IV
A2-T2	2.5	1.6	-	-	25.7	28.3	-	-	-	-	-	IV
A3-T1	3.0	1.6	-	-	29.1	38.4	-	-	-	-	-	IV
B3-T1	2.0	0.53	16.1	14.2	41.3	36.3	46.5	40.9	2.88	1.13	2.77	III
B2-T2	1.5	0.97	34.5	22.8	46.4	30.6	58.7	38.7	1.70	1.27	1.71	III
B1-T2	1.75	0.96	31.8	24.5	33.9	26.1	53.9	41.5	1.69	1.59	1.61	III
B1-T1	2.0	0.95	28.5	25.1	52.7	46.4	52.7	46.4	1.85	1.0	1.68	III
B2-T1	3.0	1.0	18.9	24.9	32.0	42.3	32.0	42.3	1.70	1.0	1.54	II
C3-T2	1.5	1.6	-	-	56.0	37.0	78.8	52.0	-	1.41	1.24	V
B3-T2	1.75	1.54	-	-	43.7	33.6	60.7	46.7	-	1.39	1.20	IV
C3-T1	3.0	1.60	31.8	42.0	39.8	52.5	39.8	52.5	1.25	1.0	1.18	III
C1-T2	1.75	2.03	-	-	45.9	35.3	76.6	59.0	-	1.67	1.19	IV
C1-T1	2.0	2.0	-	-	55.0	48.4	64.9	57.1	-	1.18	1.14	IV
C2-T2	1.75	3.0	-	-	50.7	39.0	80.8	62.2	-	1.60	1.04	IV
C2-T1	2.0	2.96	-	-	59.7	52.5	76.2	67.1	-	1.28	1.02	IV

Table 2. Test results of Series A, B and C of ref 1.

Table 3 gives calculated values for the principal tensile stress at failure,  $\sigma_{tf}$  at the centroid of the section for those beam tests failing by diagonal cracking of the web.  $\sigma_{tf}$  is assumed to be caused by the combined action of flexure and shear. It is assumed in the calculations that the shear stress is uniform across the width of the section and that shear stress does not affect the distribution of bending stress so that:

$$\sigma_{tf} = \frac{\sigma_p}{2} - \left\{ \left( \frac{\sigma_p}{2} \right)^2 + \tau_f^2 \right\}^{0.5}, \quad \text{--- (1)}$$

where  $\tau_f = V_{cr} \frac{A_v}{Ib}$



Also given in Table 3 are calculated values for the flexural tensile strength of the masonry,  $f_{kt}$ , at the soffit of the section for the beams in which shear failure was preceded by flexural failure. In the calculation  $f_{kt}$  is assumed to be caused by flexural stresses alone, plane sections before bending are assumed to remain plane after bending and stress is assumed to be proportional to strain. Thus:

$$f_{kt} = \sigma_b - \frac{M_c}{Z_b} \quad - - - - - (2)$$

Test No.	a/d	$\sigma_p$ N/mm <sup>2</sup>	$\tau_f$ N/mm <sup>2</sup>	$\sigma_{tf}$ N/mm <sup>2</sup>	$f_{kt}$ N/mm <sup>2</sup>
A3-T2	1.5	1.6	1.39	0.8	-
A1-T1	2.0	1.59	0.82	0.35	-
A1-T2	2.0	1.59	0.81	0.34	-
A2-T1	2.5	1.59	0.77	0.31	-
A2-T2	2.5	1.6	0.74	0.29	-
A3-T1	3.0	1.6	0.84	0.36	-
B3-T1	2.0	0.53	-	-	0.22
B2-T2	1.5	0.97	-	-	0.24
B1-T2	1.75	0.96	-	-	0.34
B1-T1	2.0	0.95	-	-	0.38
B2-T1	3.0	1.0	-	-	0.32
C3-T1	3.0	1.6	-	-	0.63
C3-T2	1.5	1.6	1.62	1.0	-
B1-T2	1.75	0.96	0.98	0.61	-
B3-T2	1.75	1.54	1.27	0.71	-
C1-T2	1.75	2.03	1.33	0.66	-
C2-T2	1.75	3.0	1.47	0.6	-
C1-T1	2.0	2.0	1.6	0.89	-
C2-T1	2.0	2.96	1.73	0.79	-
D1-T1*	1.0	1.6	2.46	1.79	-
D1-T2	1.0	1.63	2.40	1.72	-
D1-T3	1.0	1.60	2.41	1.74	-
D2-T2*	1.96	1.96	0.88	0.34	-
D3-T1	4.52	1.67	-	-	0.18
D3-T3	1.0	2.96	2.93	1.80	-
E1-T1	2.0	0.56	-	-	0.28
E1-T2	2.0	1.53	0.83	0.36	-
E2-T1	2.0	1.87	0.78	0.28	-
E2-T2	2.0	2.93	1.08	0.36	-
F1-T1	3.44	2.70 <sup>†</sup>	-	-	0.31
F1-T2	1.48	3.0 <sup>†</sup>	-	-	0.15

\* Beam tests with unfilled  
perpend joints

† Comp. stress at soffit beam

Table 3. Calculated failure stresses

Test No.	$\frac{V_c \text{ exp}}{V_c \text{ the}}$	$\frac{V_{cr} \text{ exp}}{V_{cr} \text{ the}}$	$\frac{V_u \text{ exp}}{V_u \text{ the}}$
A3-T2	-	1.04	-
A1-T1	-	1.23	-
A1-T2	-	1.21	-
A2-T1	-	1.16	-
A2-T2	-	1.12	-
A3-T1	-	1.26	-
B3-T1	1.00	2.75	2.32
B2-T2	1.04	1.18	1.30
B1-T2	1.14	1.13	1.58
B1-T1	1.14	2.77	2.29
B2-T1	1.11	1.65	1.39
C3-T2	-	1.21	1.71
B3-T2	-	1.25	1.73
C3-T1	1.22	1.73	-
C1-T2	-	1.18	1.96
C1-T1	-	2.11	2.50
C2-T2	-	1.10	1.76
C2-T1	-	1.92	2.46
D1-T1	-	1.30	-
D1-T2	-	1.27	-
D2-T1	-	1.28	1.90
D2-T2	-	1.09	2.2
D3-T1	1.12*	1.21	1.21
D3-T2	-	2.40	-
D3-T3	-	1.28	1.8
E1-T1	1.13*	1.91	1.6
E1-T2	-	1.22	1.57
E2-T1	-	1.06	1.64
E2-T2	-	1.21	1.78
F1-T1	1.22	-	1.8
F1-T2	1.13	1.26	1.18

\* Including self weight

Table 4. Comparison between experiment and theory

#### 4. THEORY

The two stages considered for analytical treatment are at first cracking of the brickwork and at collapse.

##### 4.1 Cracking

Having obtained experimental values for the tensile strength of the brickwork due to bending,  $f_{kt}$ , and due to combined shear and bending,  $\sigma_{tf}$ , equations (3) and (4) can be used to predict the shear force required to cause diagonal and flexural cracking. In equation (3) the effect low  $a/d$  ratios has on enhancing the principal tensile stress at failure has been included by drawing a lower bound curve to the calculated values as shown in Figure 5. From equation (1):

$$V_{cr} = \frac{Ib}{A\bar{y}} \{ \sigma_{tf}^2 + \sigma_p \sigma_{tf} \}^{0.5}$$

where

$$\sigma_{tf} = 2.25 - a/d; \quad \max \sigma_{tf} = 1.25 \text{ N/mm}^2$$
$$\min \sigma_{tf} = 0.25 \text{ N/mm}^2$$

- - - - - (3)

From equation (2):

$$V_c = \{ \sigma_b + f_{kt} \} \frac{Z_b}{a}$$

where

$$f_{kt} = 0.2 \text{ N/mm}^2 \quad (\text{see Table 3})$$

$$V_c = \frac{M_c}{a}$$

- - - - - (4)

##### 4.2 Collapse

The tests have shown that there is always some reserve of shear strength after first cracking. After initial diagonal cracking, however, this increase may be small - as little as 18% - whereas after first flexural cracking the increase in prestress force can cause a significant increase in capacity before collapse is finally brought about by the formation of a diagonal crack. For all cases collapse occurs eventually by diagonal cracking so that equation (3) is modified to give equation (5), thus:



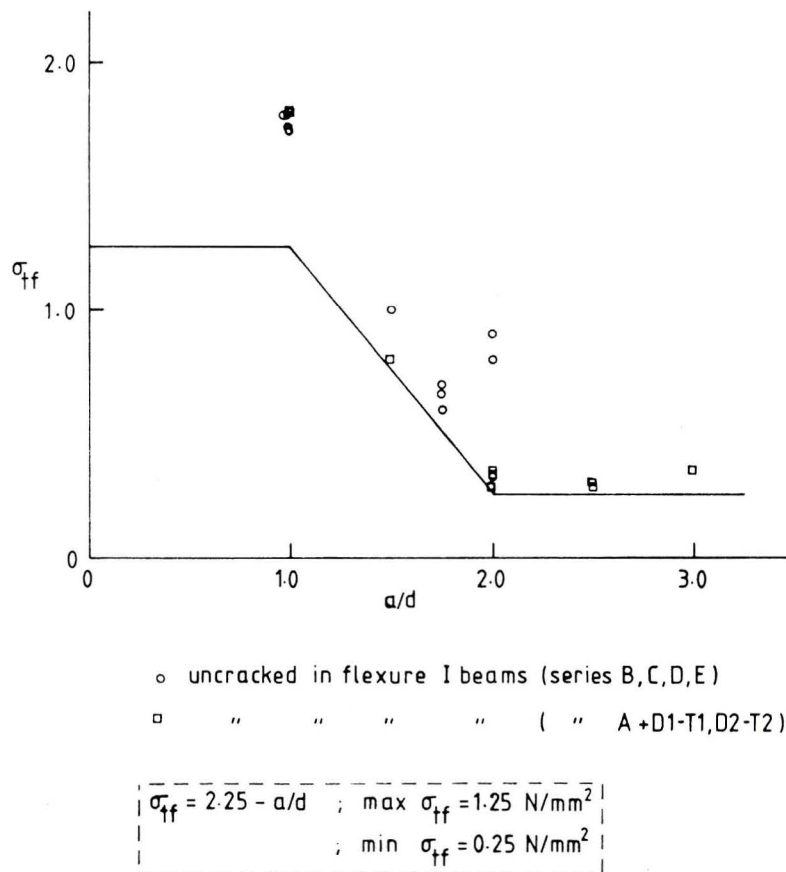


Figure 5. Effect of  $a/d$  on  $\sigma_{tf}$

$$V_u = \frac{Ib}{A\bar{y}} \{ \sigma_{tf}^2 + \sigma_{pu}\sigma_{tf} \}^{0.5}$$

where  $\sigma_{tf}$  is as for equation (3) - - - - - (5)

$$\sigma_{pu} = 2.5 \sigma_p - \sigma_p^2 ; \quad \max \sigma_{pu} = 2\sigma_p$$

$$\quad \quad \quad \min \sigma_{pu} = \sigma_p$$

$\sigma_{pu}$  is derived from Figure 6 and is a lower bound curve to the test results.

## 5. COMPARISON BETWEEN EXPERIMENT AND THEORY

In Table 4, a comparison is made between the experimental and theoretical values of shear force, as predicted by eqns (3) to (5), at cracking and ultimate. The theoretical predictions appear to be overconservative in some cases but this is to be expected since the empirical equations derived have

all been lower bound curves to the test results. These equations, however, can be safely used in design with appropriate safety factors.

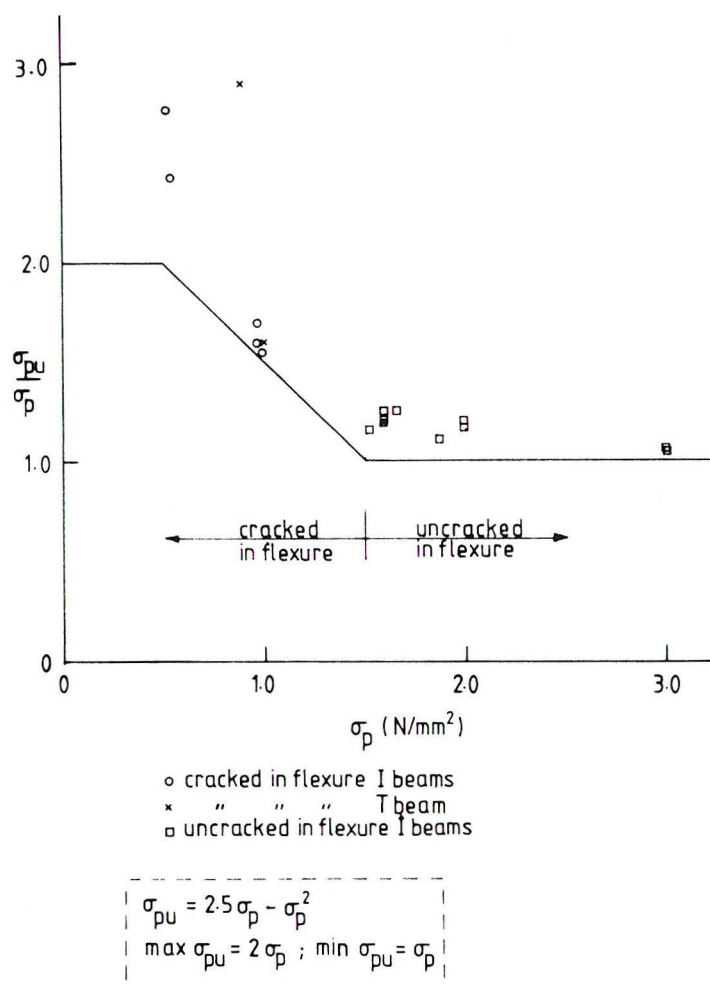


Figure 6. Increase in prestress force at ultimate

## 6. DISCUSSION

### 6.1 Effect of $a/d$

The calculated principal tensile stress to cause shear failure increases with low shear span/beam depth ratios, Figure 5. This improvement in  $\sigma_{tf}$  is only apparent and is due to the strut action which develops between load and reaction points with short shear spans. Vertical compressive stresses are induced which reduce the severity of the actual principal tensile stresses. For beam test D3-T2 for example,  $a/d = 0.5$ , the compressive stresses become so high that web shear failure was not possible with the test apparatus used. With  $a/d > 2.0$  the diagonal cracking strength remains constant.

The ultimate shear strength increases with decrease in  $a/d$ , Figure 7.

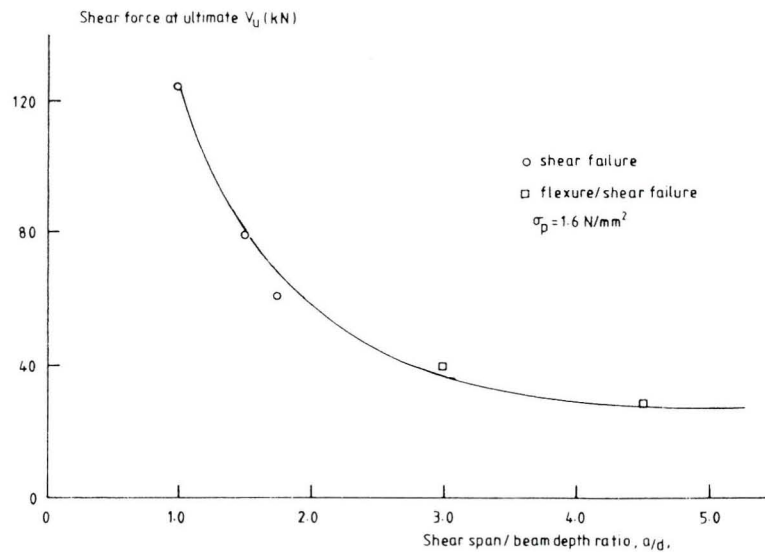


Figure 7. Effect of  $a/d$  on ultimate shear strength

## 6.2 Effect of prestress

Prestress does not affect the principal tensile stress at failure, but as seen from Figure 8, an increase in the level of prestress is accompanied by an increase in shear strength. It is also seen, Figure 9, that the amount of initial prestress, in this case concentric, affects the ultimate shear strength.

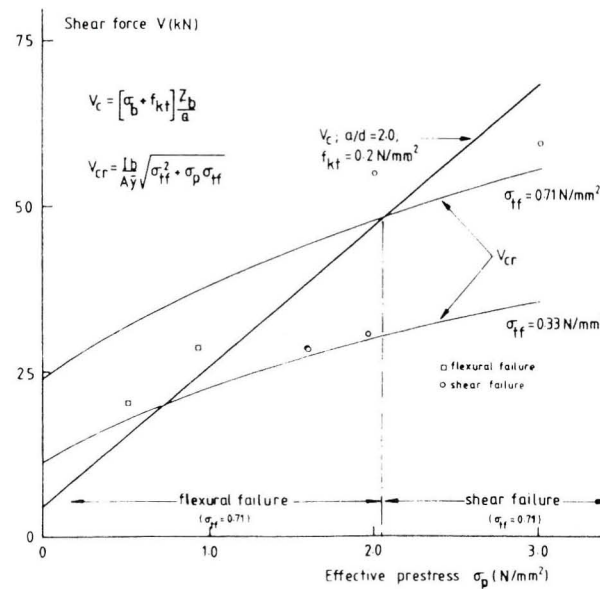


Figure 8. Moment - shear interaction diagram at cracking



As the load on the beam increases beyond the first cracking load to failure the prestress increases. This is primarily because of the change in the neutral axis position and it is mainly associated with low levels of initial prestress and flexural failures, Figure 6.

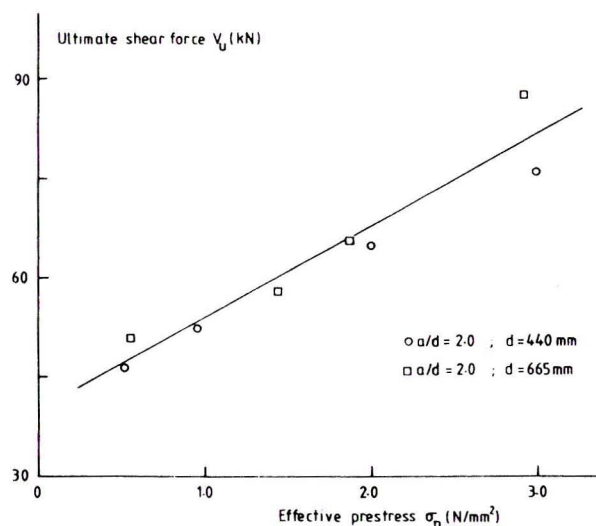


Figure 9. Effect of prestress on ultimate shear strength

### 6.3 Effect of depth

The flexural tensile strength of the deeper beams is of the same order of magnitude as the shallow beams. For the same  $a/d$  ratio and prestress levels the principal tensile failure stress of the deeper beams is close to the same level as that of the Series A shallow beams but lower than that measured in the Series C beams. This may be due to the more likely incidence of weakness in the larger number of perpendicular joints in the webs of the deeper beams or it may be because the webs of the deeper beams are subjected to less constraint from the flanges than the webs of the shallow beams.

Figure 9 compares the ultimate shear strength of the deeper beams in absolute terms with the Series B and C shallow beams and it can be seen that there is little, if any, increase in strength with increase in depth.

### 6.4 The T beam

The behaviour of the T beam was, in general, similar to the I beams. As seen from Table 1, the  $a/d$  ratio affects both the ultimate mode of failure and the strength. Initial failure, as expected, occurred always in bending.

## 6.5 The effect of open perpend joints

Open perpend joints (or cracked perpend joints in the case of Series A tests) can affect the principal tensile stress at failure. With low  $a/d$  ratios, however, this effect is reduced due to the more dominant influence of the  $a/d$  ratio. The presence of unfilled perpend joints in the web of the section does not appear to influence the ultimate shear strength of the beams.

## 7. CONCLUSIONS

7.1 At cracking, the shear strength of the beams can be related to a limiting value of principal tensile stress. This limiting value of stress increases with  $a/d$  ratios less than 2.0.

7.2 A reduction in the shear span/beam depth ratio leads to an increase in the ultimate shear strength.

7.3 The tests have shown that an increase of prestress level leads to an enhancement of the shear strength of the beams at the serviceability and ultimate limit states.

7.4 Cracks in perpend joints caused by prestressing or open perpend joints can lead to a reduction in the diagonal cracking strength of the beams but they do not appear to affect the shear strength at collapse.

7.5 Increasing the depth of the I beams from 440 mm to 665 mm did not appreciably increase their ultimate shear strength. The increase in depth caused a reduction of the diagonal cracking strength to the level of the beams with cracked or open perpend joints.

7.6 Changing the section shape of the beams from I to T shape and, as a result, using eccentric prestress caused no fundamental changes in behaviour.

7.7 The tests have identified four different types of shear failures. Collapse is usually brought about when inclined cracks penetrate into the compression flange.

7.8 Equations are presented which can be used in design to assess the shear strength at the cracking and collapse stages of both brick masonry walls such as diaphragm walls and fin walls and brick masonry I and T shaped beams and columns. The equations give satisfactory agreement with the experimental results and give safe design values.

#### ACKNOWLEDGEMENTS

The work was carried out in the Department of Civil and Structural Engineering at U.M.I.S.T. Funds for the construction of the test specimens were provided by Building Research Establishment and the Brick Development Association.

Mr. Roumani is sponsored by the Reginald Ewart Bowles Research Studentship.

#### REFERENCES

1. ROUMANI, N. and PHIPPS, M.E. "The Shear Strength of Prestressed Brickwork Sections" 8th International Symposium on Loadbearing Brickwork, British Ceramic Society, London 1983.
2. WILLIAMS, E.O.L. and PHIPPS, M.E. "The Bending Behaviour of Prestressed Masonry Box Beams at Ultimate" 6th IBMaC, Rome 1982.